RAA 2020 Vol. **20** No. **6**, 94(14pp) doi: 10.1088/1674–4527/20/6/94

http://www.raa-journal.org *http://iopscience.iop.org/raa*

***R**esearch in*
***A**stronomy and*
***A**strophysics*

Identification of temperature anomaly RR Lyrae stars in LAMOST survey, misclassification and binarities

Lin-Jia Li[1,2,3], Sheng-Bang Qian[1,2,3,4], Jia Zhang[1,2,3], Jia-Jia He[1,2,3] and Li-Ying Zhu[1,2,3,4]

[1] Yunnan Observatories, Chinese Academy of Sciences, Kunming 650216, China; *lipk@ynao.ac.cn*
[2] Key laboratory of the structure and evolution of celestial objects, Chinese Academy of Sciences, Kunming 650216, China
[3] Center for Astronomical Mega-Science, Chinese Academy of Sciences, Beijing 100101, China
[4] University of Chinese Academy of Sciences, Beijing 100049, China

Received 2019 December 16; accepted 2020 January 20

Abstract RR Lyrae stars, a well-known type of pulsating variable stars, have been known about for more than a century. A large amount of photometric data on RR Lyrae stars has been accumulated by space- and ground-based sky surveys, but the spectral data are relatively poor. Fortunately, the LAMOST sky survey project provides an opportunity to view them from the point of view of spectra. We collect the atmospheric parameters of 1685 RR Lyrae stars provided by the LAMOST catalog, and carry out research by using the reliable $T_{\rm eff}$. We find that there is a clear correlation between their $T_{\rm eff}$ and pulsation periods, which is consistent with the pulsation and evolution theories of RR Lyrae stars. In addition, we focus on those RR Lyrae stars with abnormal temperatures. After analyzing the data from several photometric surveys, we find that some of these temperature anomalies are misclassified variable stars (e.g., eclipsing binaries, pulsating stars on main sequence), and some are RR Lyrae binary candidates. For the latter, the temperatures of potential companions should be lower and their luminosities should not be neglected (e.g., red giant stars). We obtain that the ratio of temperature anomaly stars to all the sample stars is 4%, which means that the impact on the further analysis (e.g., kinematics analysis) is low. We also present the catalogs of spectral anomaly RR Lyrae stars.

Key words: techniques: spectroscopic — techniques: photometric — stars: fundamental parameters — stars: variables : RR Lyrae

1 INTRODUCTION

RR Lyrae stars (RRLs) are short period pulsation variable stars with pulsation periods ranging from 0.2 to 1.0 days (Soszyński et al. 2014; Catelan & Smith 2015). Based on the shapes of the light curves and pulsation periods, they are divided into three subtypes: a-, b- and c-type RRLs (RRa, RRb and RRc stars; Bailey 1902). The periods of RRa and RRb stars are relatively longer, the average values are 0.7 and 0.5 days, respectively. Their light curves are asymmetrical, display steep rises and gradual declines. Because both of their oscillation modes are the fundamental radial mode, commonly they are collectively called ab-type RRLs (RRab stars). The periods of RRc stars are shorter, and the mean value is about 0.3 day. This type of star shows symmetrical light curves, and its oscillation mode is the first-overtone radial mode. Some RRLs oscillating in both modes are also called d-type of RRLs (RRd stars). RRLs are the low-mass evolved stars in the core-helium burning stage. In the H-R diagram, they are located at the intersection of the horizontal branch and the classical Cepheid instability strip. The spectral types of RRLs are between A2 to F6, and the mean surface temperatures range from 7250 to 6000 K (Catelan 2004; Catelan & Smith 2015). The mean absolute optical magnitudes are in a small range ($\langle M_{\rm v}\rangle \sim 0.6 \pm 0.2$ mag). As evolved metal poor stars, their mean surface gravities are relatively smaller than those main sequence stars with similar temperatures (2.5$\sim$3.0 cm s^{-2}), and they are usually more metal poor than the Sun. The most metal poor RRLs can be down to [Fe/H] $= -2.5$. The pulsations of RRLs also induce the periodic variations in the radial velocities. The full amplitudes of radial velocity are 60$\sim$70 km s^{-1}

for RRab stars, and 30∼40 km s^{-1} for RRc stars (Smith 2004).

RRLs are widely found in the Galaxy (i.e., globular clusters, Galactic halo, thick disk and bulge) and Local Group. Comparing with other types of variable stars, RRLs have short pulsation periods ($<$1 days) and high amplitudes ($>$0.3 mag), making them able to be identified more easily by the ground-based telescopes. In recent years, several sky surveys, like ASAS (Pojmanski 1997), SDSS (Ivezić et al. 2000), NSVS (Woźniak et al. 2004), QUEST (Vivas & Zinn 2006), CRTS (Drake et al. 2009), and CATALINA (Torrealba et al. 2015; Drake et al. 2017), have successfully found large numbers of Galactic RRLs. Moreover, the sky surveys, MACHO, OGLE and VVV surveys, monitored the Galactic bulge and found tens of thousands of RRLs (Minniti et al. 1997; Alcock et al. 1998; Soszyński et al. 2014; Gran et al. 2015, 2016; Contreras Ramos et al. 2018). Recently, *Gaia* DR2 published the multi-band time-series photometry of more than 140 000 RRLs, of which more than 50 000 stars were previously undiscovered (Clementini et al. 2019). The large number and wide distribution of RRLs make them good study objects that can be used to investigate the chemical, dynamical properties and evolution of old population stars in the Galaxy and nearby galaxies (Smith 2004). However, some other types of variable stars have similar ranges of period and amplitude (e.g., eclipsing binaries), misclassification may occur in these photometric surveys, and will affect the following analysis that use RRLs as probes. Fortunately, different types of variable stars are usually located in the different positions in the H-R diagram, which mean that they have different $T_{\rm eff}$ and $\log g$. Therefore, more spectral information is necessary to identify their real types.

In the universe, binary and multiple star systems are common for stars. Compared with many other types of pulsation stars that have been found to exist in different types of stellar systems (Zhou 2010), RRLs are rarely observed in binary systems (Kervella et al. 2019 and references therein). The reasons that cause this phenomenon should be that some determined methods suffer from limitations due to the properties of RRLs (Smith 2004; Li & Qian 2014) and these stars are also not expected to exist in binary systems with short periods due to their evolutionary history (Richmond 2011[1]) unless they are binary evolution pulsators recently discovered and studied (Pietrzyński et al. 2012). The pulsations themselves can be used as probes to determine the binary nature, the corresponding mechanism is the light travel time effect (Irwin 1952), and the corresponding method is the O$-$C method (Observed mins Calculated method, Sterken 2005). Based on this method, dozens of binary systems containing RR Lyrae variables have been discovered recently by using the photometric data (Li & Qian 2014; Hajdu et al. 2015; Liška et al. 2016b,a; Sódor et al. 2017; Li et al. 2018; Prudil et al. 2019), but the ratio to all RRLs is still low. Of course, a number of projects using other different methods to detect RR Lyrae binary candidates are also proposed and carried out (Guggenberger et al. 2016; Kervella et al. 2019). Moreover, in some case, the spectra observations can provide information on the binary nature. Suppose that the companions having the similar masses with RRLs, have also evolved from main sequence, and has become red giant stars, horizontal branch stars (e.g., red horizontal branch stars, extreme horizontal branch stars, and even RRLs), or asymptotic giant branch stars, their luminosities cannot be ignored. Therefore, the RRL spectra would display different patterns. For example, if the companion was a red giant stars, the combined spectrum should show a lower effective temperature and surface gravity; if the companion was an extreme horizontal branch star (O/B subdwarfs), the spectrum would show the opposite pattern.

However, it will take a long time to accumulate enough samples by using a general telescope to observe the stars spectroscopically one by one. Fortunately, the LAMOST survey provides an opportunity for us to carry out the study. In this paper, we focus on the $T_{\rm eff}$ of RRLs provided by LAMOST. In Section 2, descriptions of the LAMOST survey and catalogs are presented. Statistical analysis of the $T_{\rm eff}$ provided by LAMOST is given in Section 3. In Section 4, we present the discussion on those temperature anomalous stars. A brief summary is given in Section 5.

2 LAMOST SURVEY AND CATALOGS

LAMOST (the Large Sky Area Multi-Object Fiber Spectroscopic Telescope, also called Guo Shou Jing Telescope) is a quasi-meridian reflecting Schmidt telescope located in Xinglong Station, National Astronomical Observatories (Wang et al. 1996; Su & Cui 2004; Cui et al. 2012; Luo et al. 2012; Zhao et al. 2012). Its effective aperture is about 3.6∼4.9 m and field of view is about 5 degree in diameter. LAMOST was designed to be able to take 4000 spectra in a single exposure to a limiting magnitude as faint as $r = 19$ at the resolution $R = 1800$ (Wang et al. 1996; Cui et al. 2012). The observation area of LAMOST covered the region $-10^\circ \leq$ Dec. $\leq 60^\circ$. After the pilot survey which started in October, 2011 and ended in June, 2012, LAMOST designed a five-year general survey which mainly focuses on the Galactic survey of stars (Luo et al. 2015). Up to August 2017, LAMOST have obtained a total of about 9 million low-resolution spectra and many scientific discoveries have been published using these data (Liu et al. 2015). Now the Phase-I LAMOST surveys have been

[1] `http://spiff.rit.edu/richmond/asras/rrlyr/rrlyr.html`

completed and the Phase-II, which will last for the next five years, includes both low- and medium-resolution spectral surveys.

There are six LAMOST catalogs: the LAMOST general catalog, the A type stars catalog, the A, F, G and K type stars catalog, the M dwarfs catalog, the observed plate information catalog and the input catalog. The LAMOST general catalog lists information such as the right ascension, declination, spectra types, redshift, $V_{\rm r}$, etc. The A, F, G and K type stars catalog provides the parameters of corresponding stars, including $T_{\rm eff}$, $\log g$, [Fe/H], $V_{\rm r}$ and their errors. In this catalog, only A type stars having high SNR spectra are included. The A type stars catalog and the M dwarfs catalog present information about the different spectral lines of corresponding stars. The observed plate information catalog and the input catalog provide the information about 4154 published plates and 4000 fiber units, respectively. It should be mentioned that, in the catalogs, a small number of stars are white dwarf stars, emission line stars, carbon stars, cataclysmic variables and spectroscopic double stars, and their spectral types are marked as WD (or WDMagnetic), EM, Carbon, CV and DoubleStar, respectively. The huge spectra and data given by LAMOST allow researchers to make statistical analysis for different type of stars, and to make new discoveries (M-giant star candidates, Zhong et al. 2015; Cataclysmic variables, Han et al. 2018; ZZ Ceti stars, Su et al. 2017; Mira variable stars, Yao et al. 2017; M dwarfs, Yi et al. 2014; Guo et al. 2015; early-type emission-line stars, Hou et al. 2016; UV emission stars, Bai et al. 2018; WD-MS binaries, Ren et al. 2014, 2018; Very metal poor stars, Li et al. 2018; EW-type eclipsing binaries, Qian et al. 2017; EA-type eclipsing binaries, Qian et al. 2018a; delta Scuti pulsating stars, Qian et al. 2018b; gamma Doradus pulsating stars, Qian et al. 2019a; RR Lyrae pulsating stars, Yang et al. 2014 and other more research, Zhang et al. 2018; Fang et al. 2016, 2018; Qian et al. 2019b).

We used delta $\sqrt{\Delta\alpha^2+\Delta\delta^2} < 2$ arcsec as decision conditions, compared the equatorial coordinates between the A, F, G and K type stars catalog and VSX (the international variable star index, Watson et al. 2006), and found that up to DR5Q3, LAMOST has obtained 6895 spectra of 4706 RRLs. Among them, 6127 spectra have been determined the spectral types, including 4290 spectra of 2984 RRab, 1649 spectra of 1146 RRc and 188 spectra of 132 RRd. Moreover, the atmospheric parameters ($T_{\rm eff}$, $\log g$, [Fe/H] and $V_{\rm r}$) of 2142 spectra are given, including 1847 spectra of 1435 RRab, 274 spectra of 231 RRc and 21 spectra of 19 RRd stars. It is worth mentioning that in VSX, the types of some variable stars are not clear, and labeled as two or more different types (e.g., RRab/EC/ESD). These objects are not included in our list, only those stars marked as RRab, RRc and RRd are selected. To evaluate the completeness of our samples, we compare them with those RRLs in VSX. Figure 1 provides the pulsation period distributions, in which the abscissa is the pulsation period, and the ordinate is the percentage of the star number. In the left panel, the period distribution of the 4706 RRLs that observed by LAMOST is similar to the distribution of the RRLs in VSX. However, in the right panel, for those 1685 RRLs that have the atmospheric parameters, the proportion of RRc with short period in LAMOST sample is smaller than the VSX sample, and that of RRab with a period greater than 0.55 days is larger. The reason for this phenomenon should be related to the sky patrol area designed by LAMOST. Because of the design of the LAMOST project, most of the observed objects, including RRLs, are in relatively high galactic latitudes. Therefore, our samples are more likely to be of the RRLs with longer periods and older ages in the galactic halo.

3 EFFECTIVE TEMPERATURE OF RRLS

For stars on the main sequence and red giant branch, LAMOST can obtain more credible atmospheric parameters, and many works based on these data have been published. However, for horizontal branch stars (RRLs, blue horizontal branch stars), there may be existing systematic deviations in the atmospheric parameters provided by LAMOST (e.g. over-estimate the [Fe/H] and $\log g$, Wu et al. 2011; Wei et al. 2014). In the four parameters provided by LAMOST, $T_{\rm eff}$ is considered to be the most accurate (Luo et al. 2015). In this paper, we carry out our research by using this parameter. Figure 2 shows the relationship between the pulsation periods $P_{\rm pul}$ and $T_{\rm eff}$ of RRLs. The green dots represent RRc, the red dots represent RRab, and the hollow green and red dots represent the objects with low $T_{\rm eff}$. There are reasons for these temperature anomalies, which will be discussed specifically in Section 4. It is generally believed that the red and blue boundaries of the pulsating instability zone of RRLs correspond to $(B-V)_0 = 0.40$ and 0.18, respectively; and the corresponding $T_{\rm eff}$ range from 7400 and 6100 K (Smith 2004). From Figure 2, it can be seen that the $T_{\rm eff}$ of LAMOST RRLs are in this range and it can also be found that the $T_{\rm eff}$ decrease with the increase of $P_{\rm pul}$. The dashed line is a parabolic fitting of all RRL data, and the result gives

$$T_{\rm eff} = 7320(80) - 1620(340)P_{\rm pul} + 302(330)P_{\rm pul}^2. \quad (1)$$

The dotted line is an arbitrary line, separating RRLs with normal $T_{\rm eff}$ from those low $T_{\rm eff}$ objects (moving the dashed line vertically downwards 450 K). After removing those low $T_{\rm eff}$ stars, we use a parabola fitting formula to fit the

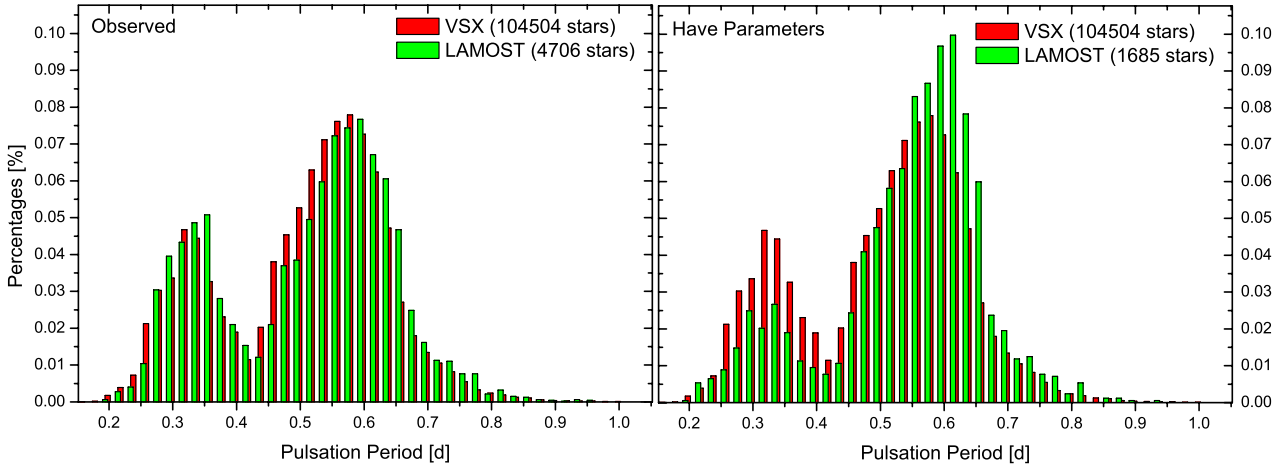

Fig. 1 Pulsation period distributions of RRLs. *Red* and *green histograms* represent RRLs collected by VSX and observed by LAMOST, respectively.

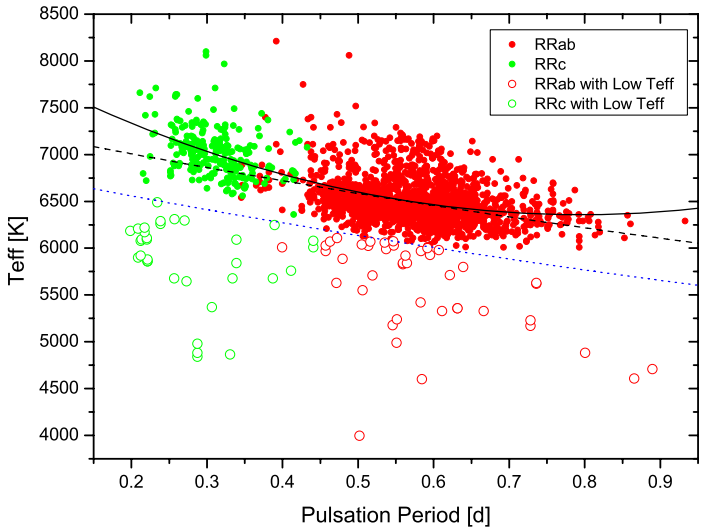

Fig. 2 Correlation between $P_{\rm pul}$ and $T_{\rm eff}$ for RRLs in LAMOST catalog. The *solid line* indicates that there is a good correlation between $P_{\rm pul}$ and $T_{\rm eff}$ for normal RRLs.

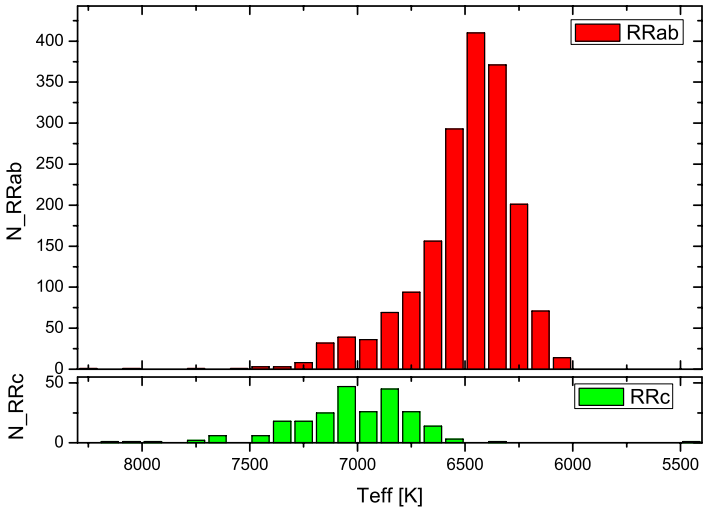

Fig. 3 Distributions of $T_{\rm eff}$ for the RRab and RRc stars. The $T_{\rm eff}$ of the latter is higher than that of the former.

remaining normal $T_{\rm eff}$ points, and the result is:

$$T_{\rm eff} = 8108(70) - 4410(280)P_{\rm pul} + 2780(270)P_{\rm pul}^2. \quad (2)$$

The solid line in Figure 2 is the corresponding fitting curve. It should be pointed out that the parameters ($T_{\rm eff}$, $\log g$, $V_{\rm r}$, etc.) are not the average values of the stars, but the values corresponding to a certain pulsation phase. This will cause the vertical dispersion of data points in Figure 2. But in some ways, the dispersion reflects the $T_{\rm eff}$ variation amplitudes in the pulsation. It can be seen that for RRc, the mean $T_{\rm eff}$ decrease with the increase of $P_{\rm pul}$, but the change of the $T_{\rm eff}$ amplitude is not significant; for RRab, the variation amplitude decreases with the increase of the pulsation period, consistent with the known behavior of RRab stars in the Bailey diagram (Smith 2004; Catelan & Smith 2015). Figure 3 shows the $T_{\rm eff}$ distributions of RRab and RRc stars. The asymmetry of RRab distribution should be due to the asymmetry of light curve. Because of the more symmetric light and $T_{\rm eff}$ curves of RRc stars, their distribution can be described by a Gauss function, and the peak value corresponds to 6980 ± 20 K.

4 DISCUSSION

In the H-R diagram, RRLs are located in a definite position, so the range of their mean $T_{\rm eff}$ values are relatively clear (range from 7400 to 6100 K). The $T_{\rm eff}$ of most RRLs provided by LAMOST are consistent with this range. Moreover, there is a certain correlation between their $P_{\rm pul}$ and $T_{\rm eff}$. According to evolution theory, the radii of the horizontal branch stars increase gradually with the helium combustion in the core, and in H-R diagram, they evolve toward to the asymptotic red giant branch in the upper right direction. In this process, the densities of stars decrease with the increase of radii. At the same time, if the stars inside the Instability Strip, their pulsation periods would increase according to the pulsation equation $P_{\rm pul}\sqrt{\bar{\rho}/\bar{\rho}_\odot} = Q$, where $\bar{\rho}$ and $\bar{\rho}_\odot$ are the values of the mean density of the star and Sun, respectively, and Q is the pulsation constant (Preston 1961). Therefore, the evolved RRLs should show longer pulsation periods, lower temperatures and higher luminosities. This is indeed reflected in Figure 3.

However, in the $P_{\rm pul}$ - $T_{\rm eff}$ diagram, we note that compared with common RRLs, a few stars show lower $T_{\rm eff}$ (39 RRab, 23 RRc, and 5 RRd stars). The similar phenomena have also been noticed in studies of other types of pulsating variables (Qian et al. 2018b). Several signs indicate that these stars are more or less related to the binarities. In the following subsections, we will discuss these low $T_{\rm eff}$ RRab, RRc and RRd stars.

4.1 Low $T_{\rm eff}$ RRab Stars

According to the criterion, 39 RRab stars are found to have lower $T_{\rm eff}$. Some RRab stars in the $P_{\rm pul}$ - $T_{\rm eff}$ diagram are located near the low $T_{\rm eff}$ limit of the normal RRab stars, and they may be also normal RRab stars. For this reason, we select 14 RRab stars with significantly lower temperatures ($T_{\rm eff}$ <5500 K) for verification. Using the photometric data provided by CRTS and Kolesnikova et al. (2008), we find that the light curves of 10 stars show typical RRab characteristics, while the variable type of remaining four stars are uncertain.

The pulsation parameters of those 10 RRab stars are summarized in Table 1, and their phased light curves are plotted in Figure 4. The rapid increases of light and relatively slow decreases indicate that they are typical RRab stars. But there are two stars worth mentioning:

CSS_J050743.8+170417 CRTS provides two groups of light curves that were observed by two different telescopes: CSS and MLS[2]. The light curves provided by MLS show no variation, and those observed by CSS, as shown in Figure 4, are diffuse. In this paper, we initially tend to classify it as an RRab star, but suggest that more monitoring are needed to confirm its pulsation type.

CSS_J163517.2+084808 Its light curve profile is different with other RRab stars. One obvious difference is that its phase of light minimum, $\sim$0.7, is earlier than that of other stars. Also noting that the bump in the middle of the descending branch of the light curve, we find the light curve of CSS_J163517.2+084808 is similar with OGLE-BLG-RRLYR-02792 (see Fig. 5). The latter is considered to be a binary evolution pulsator in classical instability strip of RR Lyrae (Pietrzyński et al. 2012; Smolec et al. 2013). Therefore, CSS_J163517.2+084808 may have a similar evolutionary process (Karczmarek et al. 2017).

As we mentioned in the introduction, the low $T_{\rm eff}$ in RRLs may be caused by the existing of a low temperature companion star whose luminosity cannot be neglected. If this is true, the additional luminosity will reduce the amplitude of the host variable stars. In Figure 6, we plot the $P_{\rm pul}$ - Amp diagram for the 10 stars. It can be seen that, except CSS_J223908.5+083841, the amplitudes of most stars are relatively less than common RRab stars. Therefore, the amplitudes ranges support our view more or less in another way.

We also study the remaining four stars, and discuss them separately:

CSS_J051704.4+062112 In its Fourier spectrum, we find two peaks appearing at $f_1 = 0.153112332$ d^{-1} and $f_2 = 1.15583499$ d^{-1}, of which the difference is about 1 d^{-1}. The period corresponding to the frequency f_2,

[2] `http://crts.caltech.edu/Telescopes.html`

Table 1 The pulsation parameters for the 10 low $T_{\rm eff}$ RRab stars. The pulsation parameters are calculated based on photometric data provided by CRTS and Kolesnikova et al. (2008); The spectral types and $T_{\rm eff}$ are obtained from LAMOST.

VSX No.	Star Name	Passband	$T_{\rm max}$ (HJD)	$P_{\rm pul}$ (d)	Mean Mag. (mag)	Full Amp. (mag)	Sp.	$T_{\rm eff}$ (K)
289205	CSS_J045411.2+094950	CV	2455586.6980	0.6317244(17)	15.232(2)	0.160(8)	F9	5360(240)
289233	CSS_J050743.8+170417	CV	2453731.8232	0.5512977(46)	15.138(27)	0.529(173)	F9	5240(220)
289300	CSS_J063209.3+481802	CV	2453715.1561	0.5018871(14)	15.604(5)	0.380(23)	K7	4000(240)
289399	CSS_J074137.5+203242	CV	2453470.2549	0.6663435(25)	17.199(6)	0.406(19)	F0	5330(450)
380230	CSS_J104515.5+105943	CV	2455924.3624	0.6311216(20)	15.974(4)	0.267(16)	F6	5360(140)
294294	CSS_J163517.2+084808	CV	2453467.1157	0.5509263(13)	15.738(3)	0.349(10)	G7	4990(120)
296583	CSS_J223908.5+083841	CV	2456461.9585	0.5458571(8)	14.712(5)	0.874(21)	F2	5180(40)
296670	CSS_J224923.3+284637	CV	2453708.9831	0.6111176(26)	14.649(3)	0.194(9)	G8	5330(80)
320423	LINEAR 11335574	CV	2454939.3591	0.5827333(12)	15.903(3)	0.317(14)	K0	5420(240)
183923	V3154 Oph	pg	2442876.5744	0.5844813(31)	16.395(18)	0.374(69)	K0	4600(190)

Notes: The Passband column contains: CV - wide band V mag; pg - photographic.

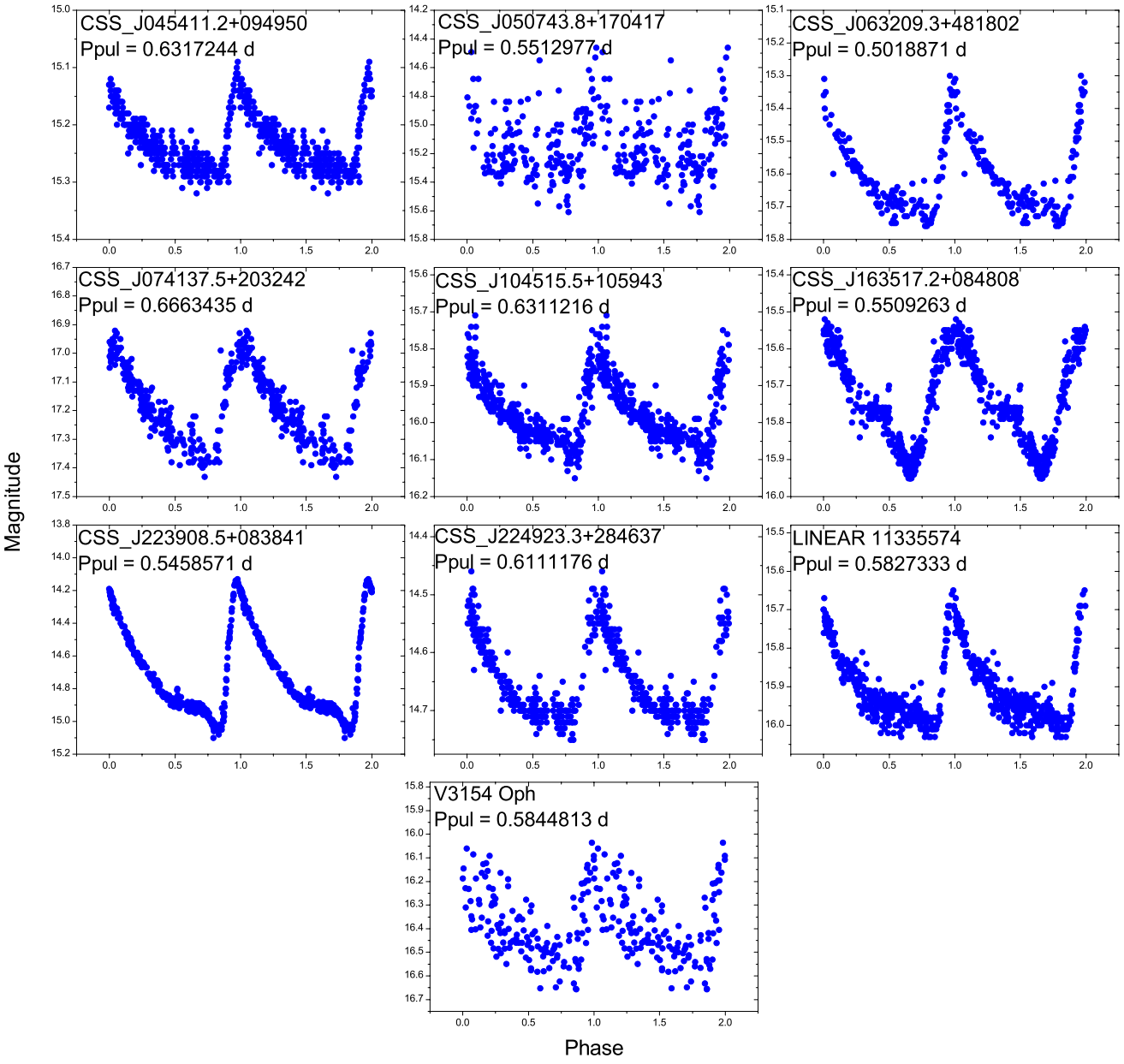

Fig. 4 The 10 low $T_{\rm eff}$ pulsation stars that can be classified as RRab star. The light curves of V3154 Oph are obtained from Kolesnikova et al. (2008), and the others are from CRTS.

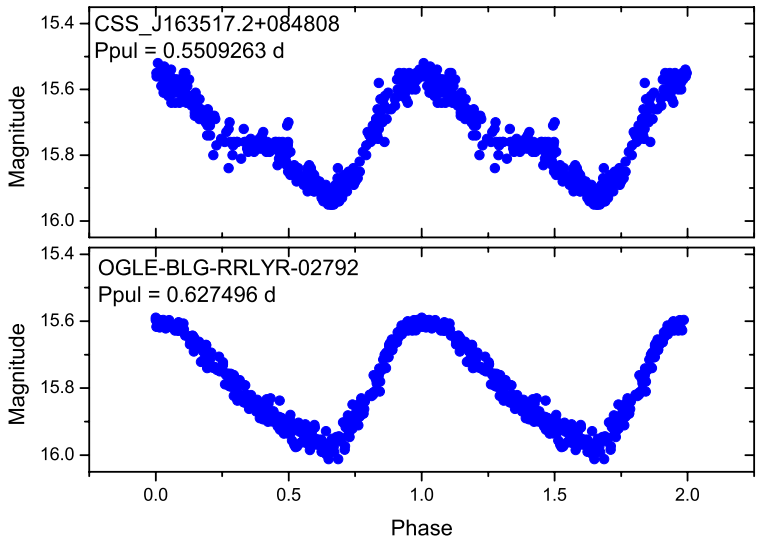

Fig. 5 The phased light curves of CSS_J163517.2+084808 and OGLE-BLG-RRLYR-02792.

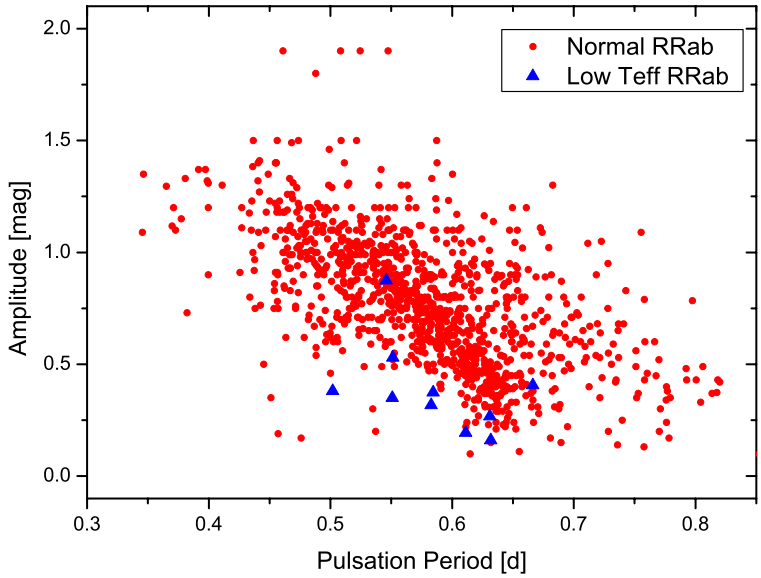

Fig. 6 The $P_{\rm pul}$ - Amp. diagram for RRab stars. *Triangles* indicate the 10 low $T_{\rm eff}$ RRab stars.

0.8651754 d, is consistent with the result given by VSX, and is within the period range of RRab stars. However, the corresponding phased light curves, as shown in the upper-left panel of Figure 7, does not show any characteristic of RRab. Considering its absolute magnitude $M_{Gaia} = 4.64 \pm 0.66$ mag (Gaia Collaboration et al. 2018), we tend to think that it is an eclipsing binary with double period (see the upper-middle panel of Fig. 7).

CSS_J061938.5+593653 Its light curve points provided by CRTS are not many, and it seems that there is a long-term change in the light curves (see the upper-right panel in Fig. 7). We did not find any significant peak in its Fourier spectrum. Noting its luminosity $L_{Gaia} = 1.919\ L_{\odot}$ provided by *Gaia* Dr2 (Gaia Collaboration et al. 2018), at least we can make sure it is not an RRab star. Maybe more monitoring is needed to reach a conclusion on this star.

MLS_J073050.1+180445 As shown in the lower-left panel of Figure 7, its phased light curves are symmetrical. The change of light increase is equal with the decrease. Therefore we exclude this star from RRab stars.

MLS_J082308.5+172823 It seems that its light curves show long-term changes. After subtracting that component, we find the highest peak in the Fourier spectrum is around $f_0 = 0.246973392\ \mathrm{d}^{-1}$. The period of 0.800505 d provided by VSX, corresponds to $1.24921143\ \mathrm{d}^{-1}$, which is about equal to $1 + f_0$. The phased light curves calculated with VSX period are shown in the lower-right panel of Figure 7, and no RRab star feature is found in it.

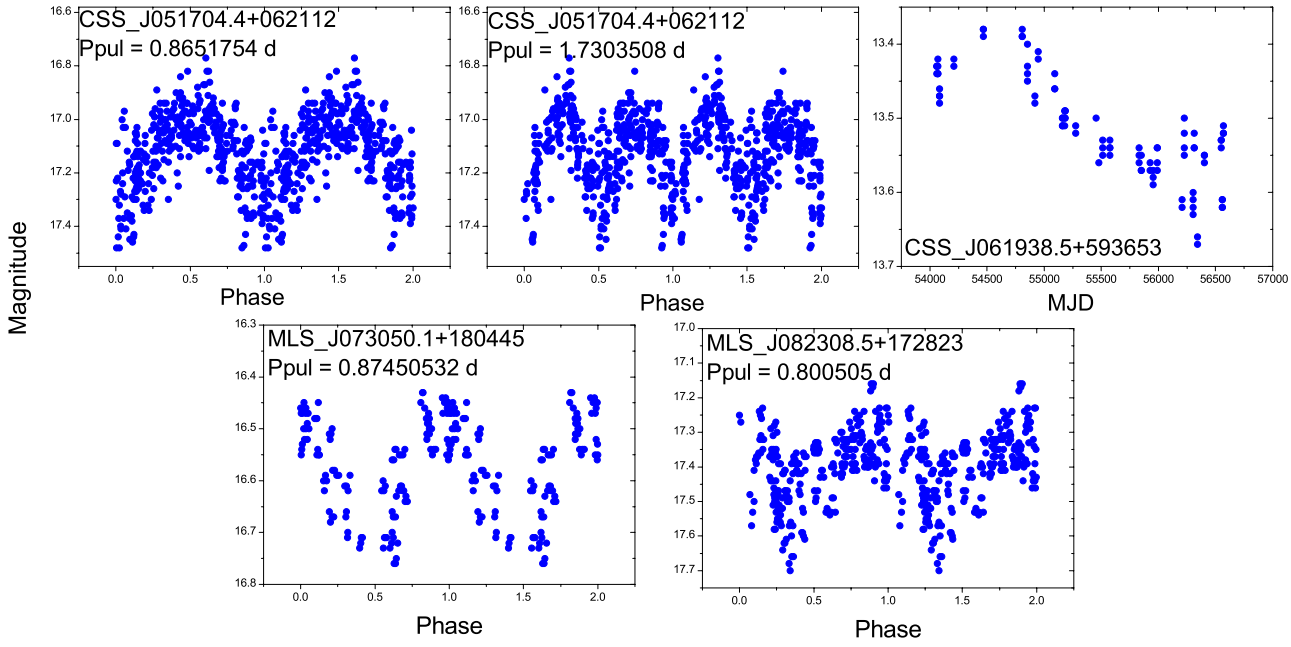

Fig. 7 The light curves for the remaining four uncertain low $T_{\rm eff}$ pulsation stars.

Table 2 The orbital or pulsation parameters for the 20 low $T_{\rm eff}$ stars originally classified as RRc stars. The orbital or pulsation parameters are calculated based on photometric data provided by sky surveys (see the Source column). The spectral types and $T_{\rm eff}$ are obtained from LAMOST.

VSX No.	Star Name	$T_{\rm min}$ (HJD)	$P_{\rm orb}$ (d)	Mean Mag. (mag)	Full Amp. (mag)	Sp.	$T_{\rm eff}$ (K)	Source
10 eclipsing binaries								
361205	CSS_J004408.4+415722	2453643.8180	0.5143273(20)	14.211(3)	0.089(9)	F8	6310(120)	CRTS
366430	CSS_J034928.1+293530	2454907.2638	0.8227828(37)	13.928(4)	0.175(12)	F9	5760(50)	CRTS
369310	CSS_J045411.8+110017	2454110.7348	1.579405(13)	12.817(5)	0.239(16)	G0	6050(130)	CRTS
372012	CSS_J054833.0+025811	2454532.6590	0.4255974(9)	15.560(6)	0.291(18)	F5	6300(120)	CRTS
138336	ROTSE1 J134533.06+234118.4	2454159.7781	0.3623975(599)	11.773(1)	0.058(3)	G3	5870(20)	SWASP
138397	ROTSE1 J143129.82+311010.8	2454268.4347	0.4177062(156)	12.361(1)	0.140(4)	G3	5900(10)	SWASP
138643	ROTSE1 J163819.95+380410.4	2454261.8457	0.4244474(12)	11.447(8)	0.271(31)	F6	6000(190)	CRTS
138630	ROTSE1 J164519.45+284021.0	2454258.8438	0.4175779(4)	13.785(4)	0.414(11)	F0	6210(160)	CRTS
230861	V0384 UMa	2456067.7620	0.4351324(14)	13.561(7)	0.223(22)	F6	6200(100)	CRTS
142231	V0504 Hya	2456588.9554	0.3795364(5)	13.920(3)	0.230(9)	F5	6490(370)	CRTS
4 RRc stars		$T_{\rm max}$ (HJD)	$P_{\rm pul}$ (d)					
361541	CSS_J005830.9+380355	2454772.7042	0.3306227(5)	15.812(4)	0.369(11)	K1	4870(20)	CRTS
362247	CSS_J012628.6+362217	2453686.7632	0.3872661(17)	17.489(9)	0.320(25)	G4	5680(340)	CRTS
395888	CSS_J223241.2+042113	2453567.8719	0.3897486(6)	14.366(4)	0.409(10)	A6V	6250(310)	CRTS
144161	FASTT 1511	2455059.8338	0.2729393(2)	14.139(3)	0.451(9)	G2	5650(380)	CRTS
6 uncertain variable stars								
417993	2MASS J04134189+3015442	2457378.4858	0.1983713(9)	16.658(6)	0.108(20)	F5	6180(300)	CRTS
270122	BEST F2_09401	2452195.5226	0.3336039(163)	12.334(1)	0.090(3)	G8	5680(10)	SWASP
163489	NSVS 12551559	2451491.2974	0.3066699(561)	12.391(7)	0.128(21)	G8	5370(60)	NSVS
300387	V0553 Ser	2453869.0214	0.2137601(19)	12.203(9)	0.129(29)	G0	6090(10)	ASAS
138435	ROTSE1 J144914.31+262451.0	2453870.8340	0.2205187(15)	11.392(5)	0.082(15)	G0	6100(20)	ASAS
75330	ASAS J032337+1540.0	2452622.2883	0.2384660(24)	9.743(5)	0.066(15)	G2	6280(20)	ASAS

4.2 Low $T_{\rm eff}$ RRc Stars

The hydrogen shells of RRc stars are relatively thinner, and their mean surface $T_{\rm eff}$ are higher than those of RRab stars. In the $P_{\rm pul}$ - $T_{\rm eff}$ diagram, we find that the $T_{\rm eff}$ of 23 RRc stars are lower than those of common RRc (the lowest $T_{\rm eff}$ one is BU UMa, $T_{\rm eff} = 4840 \pm 40$ K, and the spectral type is G7). In addition, it can been seen that more low $T_{\rm eff}$ RRc stars are concentrated to short pulsation period around $0.25 - 0.3$ d (see Fig. 3). Qian et al. (2018b) studied the δ Scuti stars in LAMOST survey, found more than 100 long-period δ Scuti stars with low $T_{\rm eff}$, and point-

ed out that some of them may actually be contact binaries having double periods. The situation of these short-period RRc stars with low $T_{\rm eff}$ should be similar. Therefore, we collect the photometric data of these 23 stars from CRTS, SWASP, ASAS and NSVS surveys to check their properties. After Fourier analysis, the results show that the light curves of 20 stars show obvious changes, in which 10 stars show obvious eclipse binary characteristics, six stars show the variations similar to other pulsation stars (e.g., δ Scuti stars, or γ Dor stars), and only four stars show typical RRc properties.

The phased light curves of 10 stars which actually are binary stars are presented in Figure 8, and the corresponding parameters, including the times of light minimum, orbital periods, amplitudes are listed in Table 2. The orbital periods of six stars are twice the values provided by VSX. The remaining four stars (CSS_J045411.8+110017, CSS_J054833.0+025811, ROTSE1 J134533.06+234118.4 and V504 Hya) show the periods that are different from those given by previous literature. From the light curves, most of them are contact binaries. Moreover, in Figure 8, it can be seen that the light curves of some eclipse binaries show O'Connell effect (the heights of the primary and second light maxima are unequal, O'Connell 1951; Milone 1968), which indicates the existence of the stellar activities in binary stars (Liu & Yang 2003).

In remaining 10 stars showing light curve variations, four stars can be identified as RRc (see Fig. 9), but the types of the other six stars need further confirmation. Figure 10 displays their phased light curves. In the upper panels, the light curves of the three stars (2MASS J04134189+3015442, BEST F2_09401 and NSVS 12551559) are similar with those peculiar δ Scuti stars (i.e., V1719 Cyg, V798 Cyg and V974 Oph, Poretti & Antonello 1988), which show asymmetry with the descending branch steeper than ascending branch. Using the *Gaia* Dr2 data (Gaia Collaboration et al. 2018), we obtain the luminosities of two of three stars: 0.516 $L_{\odot}$ for BEST F2_09401 and 1.02 $L_{\odot}$ for NSVS 12551559, suggesting that they are probably special δ Scuti stars on the main sequence. However, in H-R diagram, the positions of these two stars closing to the location of Sun, are far beyond the red edge of δ Scuti variables. Moreover, their absolute magnitudes are larger than those previous discovered peculiar δ Scuti stars. In the study on δ Scuti stars in LAMOST, Qian et al. (2018b) have detected a group of 131 unusual and cool variable stars. In those stars, some stars are actually eclipsing binaries, but misclassified, just like the stars in Figure 8. But there are also some stars which may be a new type of pulsating star (Qian et al. 2018b). The observations and investigations on these "peculiar" pulsating stars may shed light on pulsation theories on solar-type stars.

The light curves of the three stars in the bottom panels of Figure 10 are more symmetrical, the phases of light minimum are around 0.5. We also obtain their luminosities from *Gaia* Dr2 data, the results are 2.51 $L_{\odot}$ for V553 Ser, 7.82 $L_{\odot}$ for ROTSE1 J144914.31+262451.0, and 4.98 $L_{\odot}$ for ASAS J032337+1540.0. Considering their temperatures and luminosities, these three stars may be γ Dor stars that have just evolved from the main sequence. However, noting that their light curves data are diffuse, the possibility that they are eclipse binaries cannot be excluded, and high-precision observation are required in the future to check their nature.

In addition to the 20 variable stars discussed earlier, we also study the remaining three stars (CSS_J085231.6+474221, BU UMa and HL Com). First of all, the light curves of CSS_J085231.6+474221 seem to show variations, but not significant. Therefore its type cannot be determined. The reason for this result may be due to its faint magnitude ($V = 16.85$ mag). For BU UMa, Wils et al. (2006) pointed out that it may not be a variable star, and Ting et al. (2018) also classified it as a red clump star. According to *Gaia* Dr2 data, the luminosity of BU UMa is 100.5 $L_{\odot}$, which is obviously brighter than the luminosities of typical RRc stars. Therefore, BU UMa is probably a red clump star or red horizontal branch star with constant luminosity. For HL Com, it was used as comparison star in Wing (1973), and later considered as an RRc star with a period of 0.339 days by Schaefer (1979). However, we use CRTS and SWASP data to verify that there was no obvious change in the light curves (there were sudden changes in the SWASP data, but the authenticity is uncertain). The luminosity of HL Com obtained from *Gaia* Dr2 data is 2.96 $L_{\odot}$, which can at least confirm that it is not an RRc star.

4.3 Low $T_{\rm eff}$ RRd Stars

In these low $T_{\rm eff}$ RRLs, there are five stars which are classified as RRd stars in VSX. We also use the photometric data collected from CRTS and SWASP to study their properties, and find light variations in four of them. The results of Fourier analysis show that only one star (LINEAR 2122319) is the real RRd star, two stars (CSS_J021911.0+402916 and CSS_J094314.0+473048) are eclipsing binaries, and one star (CSS_J173442.1+374141) should be a type II Cepheid star with a pulsation period of about 7.023 d. Their phased light curves are plotted in Figure 11, and the corresponding pulsation or orbital parameters are listed in Table 3. The light curves of the last star, CSS_J180258.2+455831,

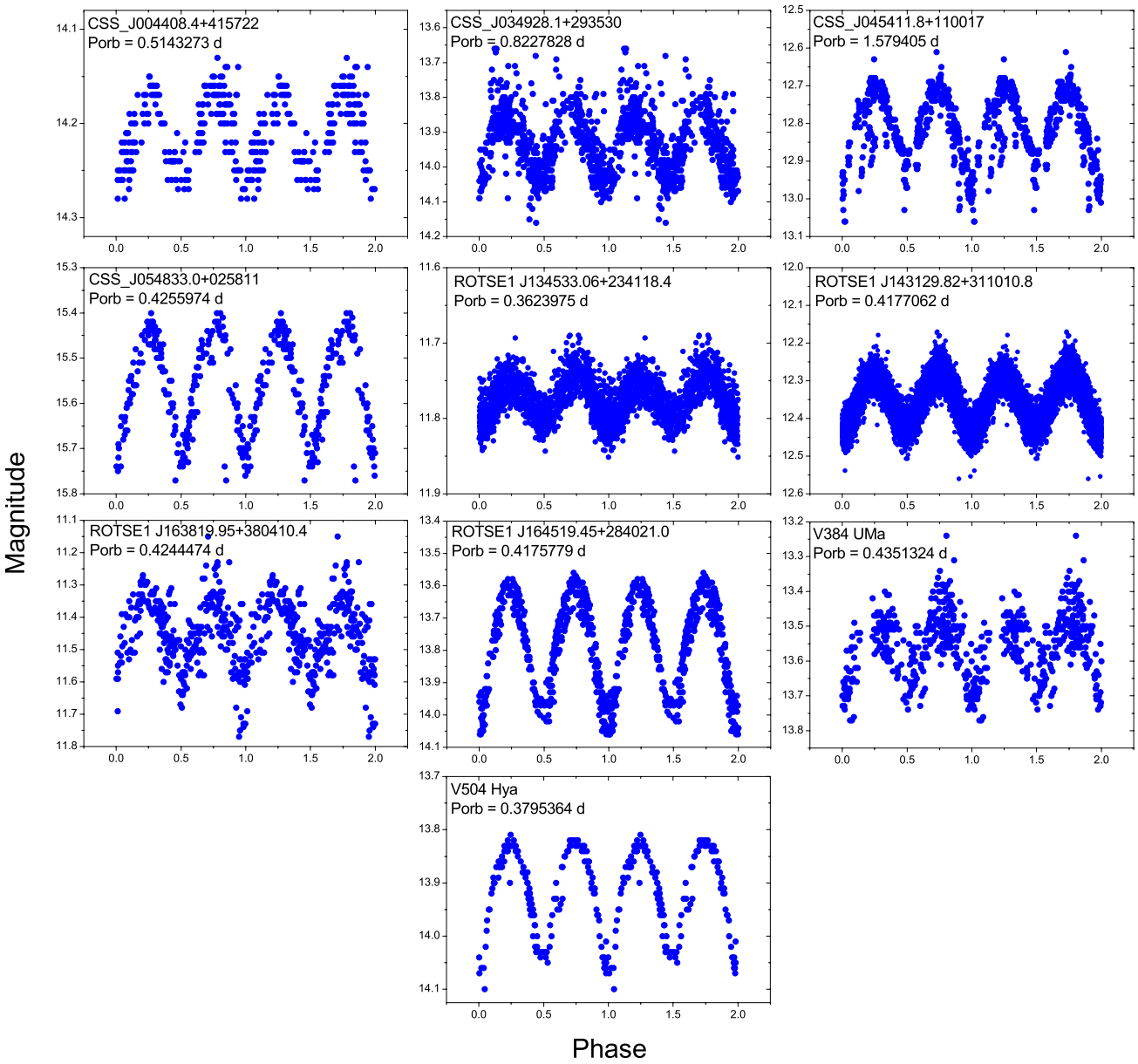

Fig. 8 The phased light curves for the 10 eclipsing binaries which were misclassified as RRc stars.

do not show any significant change. Considering the high luminosity provided by *Gaia* Dr2, 345 $L_{\odot}$, and the low $T_{\rm eff}$ and $\log g$, we conclude that it should be a red giant star.

4.4 RRLs with Abnormal Spectrum Types

In the LAMOST catalog, there are a lot of RRLs only given spectral types. We find that some of them are different from the normal RRLs in spectral types, either early or late, and even some of them are marked as binaries or CV. Although it cannot be ruled out whether there are problems during data processing, these objects are also potentially valuable and worthy of further confirmation and research. Therefore, we list their information in Table 4.

5 SUMMARY

The LAMOST catalog provides spectral information for thousands of RRLs in Galaxy. In this paper, we adopt the parameter $T_{\rm eff}$ for statistics and analysis, and obtain the following results:

1. Among the four parameters provided by LAMOST catalog for RRLs, the effective temperature $T_{\rm eff}$ is accurate and credible. Moreover, there is an obvious correlation between $T_{\rm eff}$ and $P_{\rm pul}$ (see Eq. (2)). More importantly, we find that a considerable number of temperature anomalies

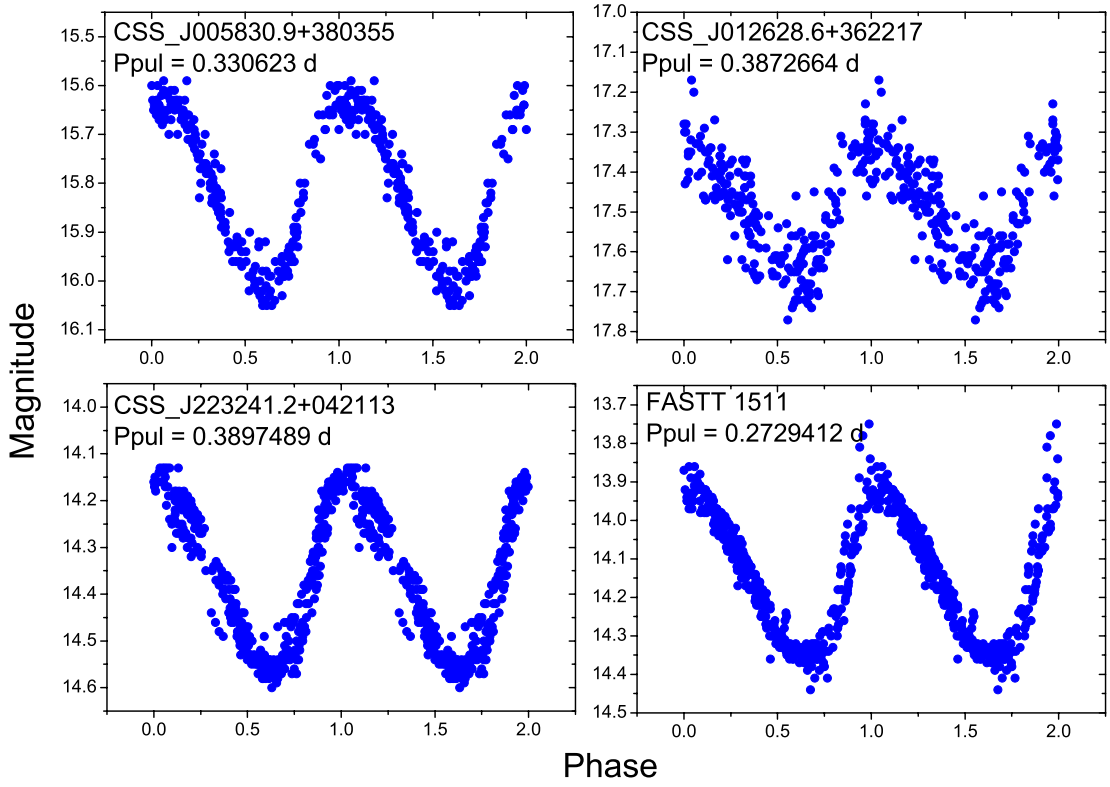

Fig. 9 The phased light curves for the four real RRc stars.

Table 3 The orbital or pulsation parameters for the four low $T_{\rm eff}$ stars which were identified as RRd stars. The parameters are obtained in the same way as the description in Table 2.

VSX No.	Star Name	$T_{\rm min}$ or $T_{\rm max}$ (HJD)	$P_{\rm orb}$ or $P_{\rm pul}$ (d)	Mean Mag. (mag)	Full Amp. (mag)	Sp.	$T_{\rm eff}$ (K)	Source
One RRd star								
318929	LINEAR 2122319		0.4825988(17) 0.3594211(5)	15.799(4)	0.185(8) 0.386(7)	G3	5670(40)	CRTS
Two eclipsing binaries								
363541	CSS_J021911.0+402916	2454418.8193	0.5171751(202)	14.526(4)	0.303(13)	F9	6140(30)	SWASP
379148	CSS_J094314.0+473048	2453793.6643	0.3615372(6)	14.303(2)	0.125(6)	F0	6320(60)	CRTS
One type II Cepheid star								
390237	CSS_J173442.1+374141	2454675.476	7.02224(15)	15.624(5)	0.181(2)	K4	4450(150)	SWASP

Table 4 The Abnormal Spectral Types for those RRLs Provided by LAMOST (the first 10 lines of the whole table)

VSX No.	Star Name	RA (deg)	DEC (deg)	Type	$P_{\rm pul}$ (d)	Date	Sp.
9694	BO Com	202.77349	16.60619	RRab	0.56376	2013–01–15	K4
9774	FH Com	201.10633	16.00203	RRab	0.74794	2016–02–16	G8
11758	V0838 Cyg	288.51571	48.19964	RRab/BL	0.4802799	2015–10–02	WD
12169	V1249 Cyg	324.40096	44.46228	RRab	0.474799	2016–11–04	G7
15235	V0424 Her	263.68275	17.95478	RRab	0.6307109	2015–04–21	G2
15572	V0761 Her	259.44661	42.23541	RRab	0.681076	2017–04–01	DoubleStar
21352	V0866 Oph	265.29087	−0.15922	RRab	0.5835579	2016–03–18	G0
22832	V2346 Oph	274.64375	8.09481	RRab	0.5905669	2017–06–12	CV
24233	V1170 Ori	83.54833	−5.92282	RRab	0.5186114	2013–11–20	M2
26471	AV Psc	16.84183	32.23522	RRab	0.47675	2014–12–19	K5

In Type column (Col. (5)), RRab/BL means that the star is an RRab star existing Blazhko effect. The Sp. column (Col. (8)) contains: WD - White Dwarf; DoubleStar - double Star; CV - Cataclysmic Variable.
The whole table is online at `http://www.raa-journal.org/docs/Supp/ms4533table04.dat`.

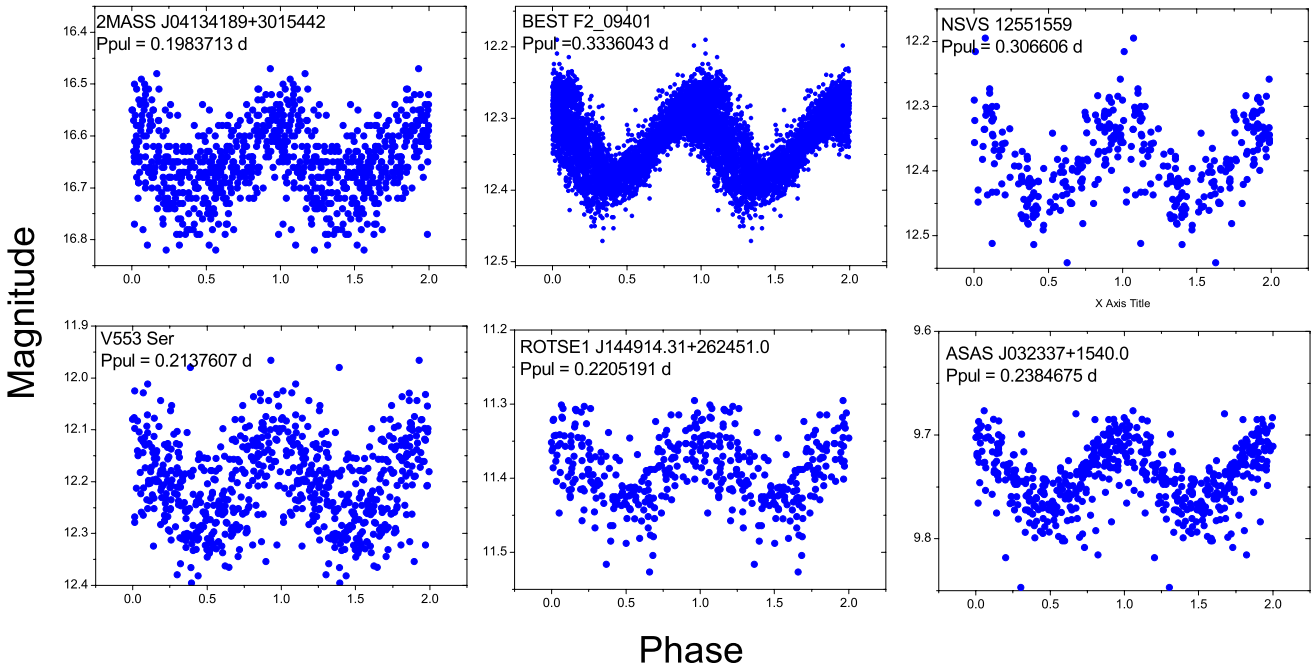

Fig. 10 The phased light curves for the six uncertain low $T_{\rm eff}$ pulsation stars.

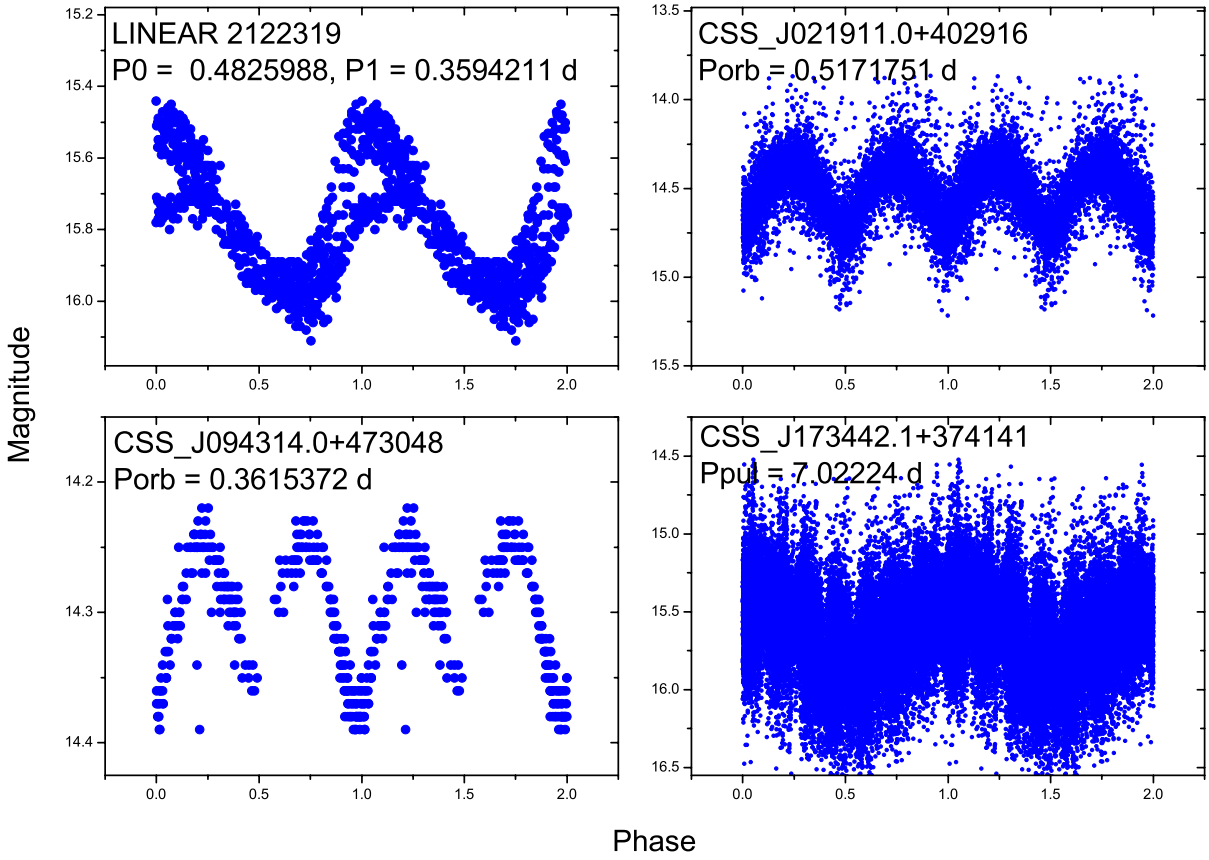

Fig. 11 The phased light curves for the four low $T_{\rm eff}$ variable stars which were identified as RRd stars. LINEAR 2122319 is folded with $P_1 = 0.3594211$ d.

exist, the ratio is about 4%. This ratio is low, and should not affect the studies on those distance determinations and kinematics analysis that use RRLs as probes.

2. The specific conditions of these temperature anomalies are also different. For the 14 anomalous RRab stars ($T_{\rm eff} < 5500$ K), most of them are certainly RRab stars, and they mostly show relatively small light amplitudes. We conclude that they may have red giant companions whose luminosity cannot be neglected. One of the stars, CSS_J163517.2+084808, shows the light curves similar to that of one of the binary evolution pulsators, OGLE-BLG-RRLYR-02792, and we speculate that it may have a similar evolution process.

For the 23 abnormal RRc stars, we confirm that 20 of them show significant light variations. After analysis, 10 of them can be considered as contact binaries, four are truly RRc stars, and six stars may be pulsating variable stars on or near the main sequence. It can be seen that most of $T_{\rm eff}$ anomaly RRc stars are misclassified.

For the five anomalous RRd stars, we find that only one is indeed an RRd star (LINEAR 2122319), while the other targets are binaries, type II Cepheid or red giant star. It can be seen that those RRLs with low $T_{\rm eff}$ are mostly related with binarities. They either are potential binary candidates with low-temperature companions or are contact binaries which are misclassified as pulsating stars. These discoveries can only be realized with the help of the massive data provided by LAMOST spectroscopic survey.

3. LAMOST provides many spectral types of RRLs, some of which marked as earlier spectral types (O and B type), and some of which are labeled as binary stars. They are also valuable research objects (see Table 4).

4. LAMOST also provides the other parameters (e.g., $\log g$, [Fe/H] and $V_{\rm r}$) for stars. But for stars on the horizontal branch, it usually overestimates $\log g$. For RRLs, it also overestimates the metal abundance [Fe/H]. Among these parameters, [Fe/H] and $V_{\rm r}$ should be the most important for studying the stellar chemical and dynamical properties of stars in the Galaxy and nearby galaxies (Maintz & de Boer 2005; Nemec et al. 2013; Fabrizio et al. 2019). We plan to reprocess the 1D spectra of RRLs, and estimate the reliable [Fe/H] values for the next research.

As a summary, the LAMOST Sky Survey project provides millions of spectral data of stars in the Milky Way. On the one hand, it has made great contributions to the study of the structure and evolution of the Milky Way, on the other hand, it has also enabled us to carry out statistical work on different types of variable stars from spectral perspective. The LAMOST project is still under way and is gradually turning to the observation of medium dispersion spectra. It is believed that in the near future, it will provide us with more abundant and accurate data. In this paper, we focus on RRLs. From the point of view of effective temperature, we find that the targets with lower temperatures are more or less related to binarities. For variable stars, spectral data is very necessary, which can make up for some deficiencies of photometric data.

Acknowledgements Guo Shou Jing Telescope (the Large Sky Area Multi-Object Fiber Spectroscopic Telescope LAMOST) is a National Major Scientific Project built by the Chinese Academy of Sciences. Funding for the project has been provided by the National Development and Reform Commission. LAMOST is operated and managed by the National Astronomical Observatories, Chinese Academy of Sciences. This work is partly supported by the National Natural Science Foundation of China (Grant Nos. 11803084, 11703082, 11325315, 11573063 and 11611530685) and the Key Science Foundation of Yunnan Province (No. 2017FA001).

This paper makes use of data from the first public release of the WASP data (Butters et al. 2010) as provided by the WASP consortium and services at the NASA Exoplanet Archive, which is operated by the California Institute of Technology, under contract with the National Aeronautics and Space Administration under the Exoplanet Exploration Program. This work has also made use of data from the European Space Agency (ESA) mission *Gaia* (`https://www.cosmos.esa.int/gaia`), processed by the *Gaia* Data Processing and Analysis Consortium (DPAC, `https://www.cosmos.esa.int/web/gaia/dpac/consortium`). Funding for the DPAC has been provided by national institutions, in particular the institutions participating in the *Gaia* Multilateral Agreement.

References

Alcock, C., Allsman, R. A., Alves, D. R., et al. 1998, ApJ, 492, 190
Bai, Y., Liu, J., Wicker, J., et al. 2018, ApJS, 235, 16
Bailey, S. I. 1902, Annals of Harvard College Observatory, 38, 1
Butters, O. W., West, R. G., Anderson, D. R., et al. 2010, A&A, 520, L10
Catelan, M. 2004, ApJ, 600, 409
Catelan, M., & Smith, H. A. 2015, Pulsating Stars (Wiley-VCH)
Clementini, G., Ripepi, V., Molinaro, R., et al. 2019, A&A, 622, A60
Contreras Ramos, R., Minniti, D., Gran, F., et al. 2018, ApJ, 863, 79
Cui, X.-Q., Zhao, Y.-H., Chu, Y.-Q., et al. 2012, RAA (Research in Astronomy and Astrophysics), 12, 1197
Drake, A. J., Djorgovski, S. G., Mahabal, A., et al. 2009, ApJ, 696, 870
Drake, A. J., Djorgovski, S. G., Catelan, M., et al. 2017, MNRAS, 469, 3688

Fabrizio, M., Bono, G., Braga, V. F., et al. 2019, ApJ, 882, 169
Fang, X.-S., Zhao, G., Zhao, J.-K., et al. 2016, MNRAS, 463, 2494
Fang, X.-S., Zhao, G., Zhao, J.-K., et al. 2018, MNRAS, 476, 908
Gaia Collaboration, Brown, A. G. A., Vallenari, A., et al. 2018, A&A, 616, A1
Gran, F., Minniti, D., Saito, R. K., et al. 2016, A&A, 591, A145
Gran, F., Minniti, D., Saito, R. K., et al. 2015, A&A, 575, A114
Guggenberger, E., Barnes, T. G., & Kolenberg, K. 2016, Commmunications of the Konkoly Observatory Hungary, 105, 145
Guo, Y.-X., Yi, Z.-P., Luo, A.-L., et al. 2015, RAA (Research in Astronomy and Astrophysics), 15, 1182
Hajdu, G., Catelan, M., Jurcsik, J., et al. 2015, MNRAS, 449, L113
Han, X. L., Zhang, L.-Y., Shi, J.-R., et al. 2018, RAA (Research in Astronomy and Astrophysics), 18, 068
Hou, W., Luo, A.-L., Hu, J.-Y., et al. 2016, RAA (Research in Astronomy and Astrophysics), 16, 138
Irwin, J. B. 1952, ApJ, 116, 211
Ivezić, Ž., Goldston, J., Finlator, K., et al. 2000, AJ, 120, 963
Karczmarek, P., Wiktorowicz, G., Iłkiewicz, K., et al. 2017, MNRAS, 466, 2842
Kervella, P., Gallenne, A., Remage Evans, N., et al. 2019, A&A, 623, A116
Kolesnikova, D. M., Sat, L. A., Sokolovsky, K. V., et al. 2008, Acta Astronomica, 58, 279
Li, H., Tan, K., & Zhao, G. 2018, ApJS, 238, 16
Li, L.-J., Qian, S.-B., & Zhu, L.-Y. 2018, ApJ, 863, 151
Li, L.-J., & Qian, S.-B. 2014, MNRAS, 444, 600
Liu, Q.-Y., & Yang, Y.-L. 2003, ChJAA (Chin. J. Astron. Astrophys.), 3, 142
Liu, X.-W., Zhao, G., & Hou, J.-L. 2015, RAA (Research in Astronomy and Astrophysics), 15, 1089
Liška, J., Skarka, M., Zejda, M., et al. 2016, MNRAS, 459, 4360
Liška, J., Skarka, M., Mikulášek, Z., et al. 2016, A&A, 589, A94
Luo, A.-L., Zhang, H.-T., Zhao, Y.-H., et al. 2012, RAA (Research in Astronomy and Astrophysics), 12, 1243
Luo, A.-L., Zhao, Y.-H., Zhao, G., et al. 2015, RAA (Research in Astronomy and Astrophysics), 15, 1095
Maintz, G., & de Boer, K. S. 2005, A&A, 442, 229
Milone, E. E. 1968, AJ, 73, 708
Minniti, D., Alcock, C., Alves, D. R., et al. 1997, Variables Stars and the Astrophysical Returns of the Microlensing Surveys, 257
Nemec, J. M., Cohen, J. G., Ripepi, V., et al. 2013, ApJ, 773, 181
O'Connell, D. J. K. 1951, MNRAS, 111, 642
Pietrzyński, G., Thompson, I. B., Gieren, W., et al. 2012, Nature, 484, 75
Pojmanski, G. 1997, Acta Astronomica, 47, 467
Poretti, E., & Antonello, E. 1988, A&A, 199, 191
Preston, G. 1961, ApJ, 133, 29
Prudil, Z., Skarka, M., Liška, J., et al. 2019, MNRAS, 487, L1
Qian, S.-B., Zhang, J., He, J.-J., et al. 2018a, ApJS, 235, 5
Qian, S.-B., Li, L.-J., He, J.-J., et al. 2018b, MNRAS, 475, 478
Qian, S.-B., He, J.-J., Zhang, J., et al. 2017, RAA (Research in Astronomy and Astrophysics), 17, 087
Qian, S.-B., Li, L.-J., He, J.-J., et al. 2019a, RAA (Research in Astronomy and Astrophysics), 19, 001
Qian, S.-B., Shi, X.-D., Zhu, L.-Y., et al. 2019b, RAA (Research in Astronomy and Astrophysics), 19, 064
Ren, J.-J., Rebassa-Mansergas, A., Parsons, S. G., et al. 2018, MNRAS, 477, 4641
Ren, J. J., Rebassa-Mansergas, A., Luo, A. L., et al. 2014, A&A, 570, A107
Schaefer, B. E. 1979, PASP, 91, 670
Smith, H. A. 2004, RR Lyrae Stars
Smolec, R., Pietrzyński, G., Graczyk, D., et al. 2013, MNRAS, 428, 3034
Soszyński, I., Udalski, A., Szymański, M. K., et al. 2014, Acta Astronomica, 64, 177
Sterken, C. 2005, The Light-time Effect in Astrophysics: Causes and Cures of the O-C Diagram, 3
Su, D.-Q., & Cui, X.-Q. 2004, ChJAA (Chin. J. Astron. Astrophys.), 4, 1
Su, J., Fu, J., Lin, G., et al. 2017, ApJ, 847, 34
Sódor, Á., Skarka, M., Liška, J., et al. 2017, MNRAS, 465, L1
Ting, Y.-S., Hawkins, K., & Rix, H.-W. 2018, ApJ, 858, L7
Torrealba, G., Catelan, M., Drake, A. J., et al. 2015, MNRAS, 446, 2251
Vivas, A. K., & Zinn, R. 2006, AJ, 132, 714
Wang, S.-G., Su, D.-Q., Chu, Y.-Q., et al. 1996, Appl. Opt., 35, 5155
Watson, C. L., Henden, A. A., & Price, A. 2006, Society for Astronomical Sciences Annual Symposium, 25, 47
Wei, P., Luo, A., Li, Y., et al. 2014, AJ, 147, 101
Wils, P., Lloyd, C., & Bernhard, K. 2006, MNRAS, 368, 1757
Wing, R. F. 1973, AJ, 78, 684
Woźniak, P. R., Vestrand, W. T., Akerlof, C. W., et al. 2004, AJ, 127, 2436
Wu, Y., Singh, H. P., Prugniel, P., et al. 2011, A&A, 525, A71
Yang, F., Deng, L., Liu, C., et al. 2014, New Astron., 26, 72
Yao, Y., Liu, C., Deng, L., et al. 2017, ApJS, 232, 16
Yi, Z., Luo, A., Song, Y., et al. 2014, AJ, 147, 33
Zhang, L., Lu, H., Han, X. L., et al. 2018, New Astron., 61, 36
Zhao, G., Zhao, Y.-H., Chu, Y.-Q., et al. 2012, RAA (Research in Astronomy and Astrophysics), 12, 723
Zhong, J., Lépine, S., Li, J., et al. 2015, RAA (Research in Astronomy and Astrophysics), 15, 1154
Zhou, A.-Y. 2010, arXiv e-prints, arXiv:1002.2729